Spatial-temporal variations of nitrous oxide emissions in coffee agroforestry systems in Costa Rica[☆]

Abeline Bentzon-Tarp [a], Diljá Helgadóttir [a], Karel Van den Meersche [b,c,d], Frédéric Gay [b,c,d], Anders Priemé [e], Olivier Roupsard [b,f,g], Carolin Mages [a], Bo Elberling [a,*]

[a] Department of Geosciences and Natural Resource Management, University of Copenhagen, Copenhagen, Denmark
[b] UMR Eco & Sols, Univ Montpellier, CIRAD, INRAE, IRD, Institut Agro, Montpellier, France
[c] Centro Agronómico Tropical de Investigación y Enseñanza (CATIE), Sede Central, no. 7.170, Cartago 30501, Turrialba, Costa Rica
[d] CIRAD, UMR Eco & Sols, Turrialba, Costa Rica
[e] Department of Biology, University of Copenhagen, Copenhagen, Denmark
[f] CIRAD, UMR Eco & Sols, Dakar, Senegal
[g] LMI IESOL, Centre IRD-ISRA de Bel Air, Dakar, Senegal

ARTICLE INFO

ABSTRACT

This study investigates spatial-temporal trends in N_2O emissions from coffee production systems in Costa Rica with a focus on the effects of nitrogen fertilisation, topography and soil type. This is done by combining *(i)* multi-year continuous dynamic chamber measurements from sites with different fertilisation levels, *(ii)* static chamber measurements taken along a typical sloping coffee field and *(iii)* measurements from a laboratory incubation experiment with nutrient addition to different soil types. In the field and in the laboratory, additions included standard NPK fertiliser, ammonium nitrate (NH_4NO_3) as well as potassium nitrate (KNO_3). Soils in a laboratory experiment were incubated under both drained and flooded conditions. Continuous measurements from automatic chambers show that annual N_2O fluxes were dominated by bursts over few weeks following N-fertilisation with peak emissions up to 60 g N-N_2O ha^{-1} day^{-1}. A two-month slope experiment with static chambers after KNO_3-fertilisation with 90 kg N ha^{-1} showed N_2O significant differences between the highest daily emission rates from the top and the bottom of the slope (134 ± 20 g N-N_2O ha^{-1} and 336 ± 104 g N-N_2O ha^{-1}, respectively) which can be explained by NO_3 transport downhill and flooded conditions favouring denitrification at the bottom of the slope. Incubation experiments indicate that denitrification is the main process controlling N_2O emissions but also that nitrification can result in low N_2O emission rates under drained conditions. It can be concluded that the reported N_2O emissions from the coffee agroforestry systems are generally low, but may be underestimated, as both poorly drained depressions functioning as N_2O hotspots as well as temporal N_2O bursts need to be taken into account.

1. Introduction

Nitrous oxide (N_2O) is a greenhouse gas (GHG) with a global warming potential almost 300 times stronger than carbon dioxide (CO_2) and contributes also to ozone depletion in the stratosphere (Myhre et al., 2013). Currently, the anthropogenic emissions of N_2O increase is mainly due to expansion of agricultural areas and the increase in the application of commercial nitrogenous fertiliser (Reay et al., 2012). Agricultural N_2O emissions account for 58% of the total human-induced emissions and N_2O emissions are estimated to increase with 35–60% by 2030

(relative to 1990) (Capa et al., 2015; Hergoualc'H et al., 2008; Reay et al., 2012; Smith et al., 2007). The N_2O emission rates are not only impacted by the amount of applied fertiliser and the timing and frequency of application, but are also influenced by precipitation, soil water content and local hydrology, soil temperatures, and nutrient availability (Liengaard et al., 2013; Zhou et al., 2016; Wang et al., 2021).

Coffee represents 7.5% of the worldwide crop production and is among the world's most valuable export commodities (FAO, 2018). Coffee is also the most intensively traded tropical agricultural commodity and is commercially cultivated in more than 50 countries in sub-

---

and tropical areas (Capa et al., 2015). In Costa Rica, coffee (*Coffea arabica*) production is one of the main drivers of economic and social development. Historically, coffee production has played a major role in the development of the country, and today coffee cultivating plantations cover an area of more than 90,000 ha, employ more than 50,000 families, encompass 145 mills, 55 roasters and 60 exporters and represent a total of 8% of the Costa Rican workforce (Danse and Wolters, 2014). The agricultural sector accounts for 37% of Costa Rica's total GHG emissions with the coffee sector being responsible for approximately 10% of the country's total GHG emissions. Roughly 25% of the GHG emissions from the agricultural sector is due to the use of synthetic fertilisers which lead to emissions of N_2O (Hergoualc'H et al., 2008). Coffee is cultivated in Costa Rica at altitudes ranging from 600 to 1600 m above sea level (m.a. s.l.) as a monoculture as well as in agroforestry systems with nitrogen-fixing shade trees (Hergoualc'h et al., 2012). Costa Rica is among the countries with the highest usage of synthetic N-fertiliser in agriculture with an average application level of 264 kg N ha^{-1} yr^{-1} generally ranging between 150 and 350 kg N ha^{-1} yr^{-1} (Hergoualc'H et al., 2008).

This study is the first to focus on both spatial and high-resolution temporal trends in N_2O emissions and a seasonal N_2O budget for a tropical agricultural system. This includes temporal variations (hot moments), variations along slopes (including intra-plot variability and hot spots) and contrasts between different soil types. The study also discusses strategies to reduce the use of fertiliser as well as to minimize the cost of fertilisers for farmers and to clarify environmental impact from the use of fertilisers across a toposequence. This includes for our study an integration of three scales: 1) process understanding on plot levels assuming 2) spatial scaling of N_2O emission on a field scale taking into account water movement and 3) regional scaling of N_2O emissions taking into account different soil types relevant for Costa Rica. The work is based on the following key research question: what are the key drivers controlling temporal and spatial trends in N_2O emissions linked to fertilisation, topography, soil types, and hydrology in Costa Rican coffee production? It is hypothesized that current estimates of annual N_2O emissions from fertilised coffee fields are biased due to (1) lack of N_2O burst measurements associated with fertilisation during and after precipitation events and (2) lack of measurements in hotspot areas for high N_2O emissions typically in depressions and other less well-drained parts of the fields.

2. Materials and methods

2.1. Study sites

Continuous N_2O and CO_2 flux measurements as well as N_2O and CO_2 flux campaigns in five plots along a slope were conducted in the "Coffee-Flux" experimental platform (Gómez-Delgado et al., 2011), located in a coffee farm on the fertile slope of the Turrialba Volcano known as Aquiares Estate Coffee (AEC). This site is further referred to as study site *I AEC* with an altitude of 1000 m.a.s.l. and a tropical humid climate where heavy precipitation rates occur even in the drier months.

Mean annual precipitation rate and mean annual air temperature (2009 – 2018) were 2820 mm and 19.5 °C with January to April being the driest months. The dominating soil type in study site *I AEC* is classified as an Andisol (Chevallier et al., 2019).

Study site *I* consisted of three separate fields (Fig. 1): Field *A* (the control) without any N fertilisation since 2012, and was exclusively fertilised with a total of 600 kg langbeinite ($K_2Mg_2(SO_4)_3$) ha^{-1} y^{-1}, such that it received similar amounts of K and Mg as the N-fertilized plots. Mean annual yield in field *A* was 15.3 tons of fresh fruit ha^{-1} (equivalent to 2.55 tons of green beans). Field *B* was fertilised three times annually with a total of 230 kg N ha^{-1} y^{-1}, under the form of granular fertiliser added by hand to the base of the coffee trees. Ammonium nitrate (NH_4NO_3) was applied after harvest (February), while a formula containing inorganic nitrogen (N), potassium (K), magnesium (Mg) and boron (B) ('*formula completa*') was applied at the beginning of fruit development (May) and at the beginning of the harvest season (September). Mean annual yield in field *B* was 16.8 tons fruit ha^{-1} (2.8 kg green beans ha^{-1}). Field *C* received the fertilisation that is practiced in the farm, which is very similar to what was applied on field *B*. Field *C* is located on a short but relatively steep slope elevating from 1049 to 1039 m.a.s.l. Along this slope, five plots were arranged equidistantly with a distance of 25–30 m with plot *I* located at the top of the slope, plot *III* located at the middle of the slope and plot *V* located at the bottom of the slope (Fig. 1).

2.2. Continuous N_2O and CO_2 flux measurements

Continuous measurements took place in study site *I*, fields *A* and *B*, from 01.04.2016 to 10.10.2018. Data of precipitation and air
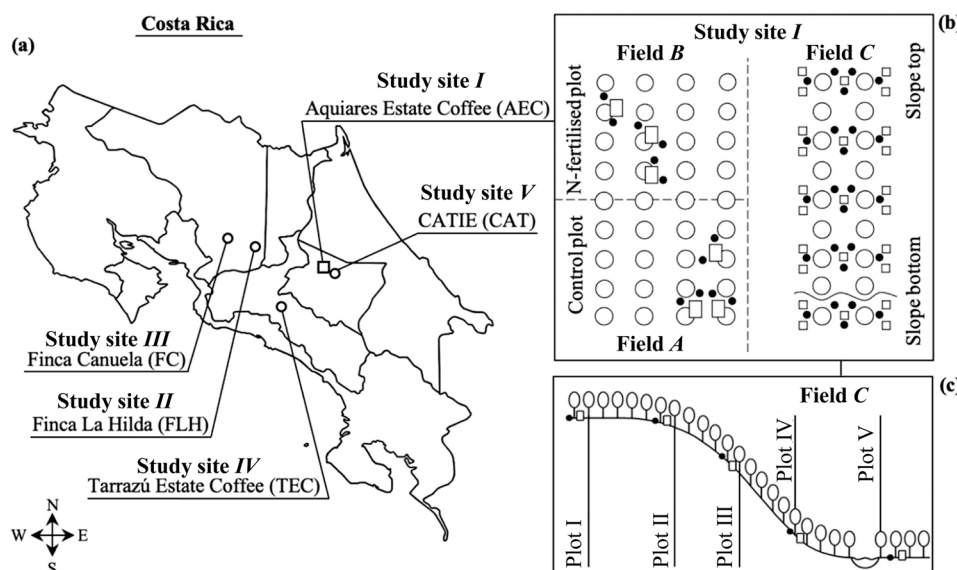

Fig. 1. (a) Map of Costa Rica with study sites marked: I -V. (b) Section of study site I in Aquiares Estate Coffee, AEC, showing the placement of the automatic measurement chambers (white squares) and location of soil sampling (black dots) in the control plot, field A and in the N-fertilised plot, field B and the static chambers (white squares), coffee plants (open circles), and location of soil sampling (black dots) in field C. Note that fields A and B are both located at the slope top (c) Cross section of field C illustrating the location of plot I – V along the slope, with plot I located at the top of the slope, plot III located at the middle of the slope, and plot V located at the bottom of the slope.

temperature were obtained from the nearby weather station managed by the collaborative platform *"Coffee-Flux"* registered as *"CR-AqC"* in *FLUXNET* and located near plot *I* at the top of the slope in field *C*. Continuous N_2O and CO_2 fluxes were measured in the control plot, field *A,* and in the N-fertilised plot, field *B*, using an automated measurement system including six steel chambers, a pump and tubing system and a N_2O and CO_2 gas analyser.

Three replicate chambers were installed in each of the fields *A* and *B*. Chamber lids were made of plexiglass sealed with rubber to ensure air tightness when closed. The lids opened and closed automatically in a slightly upward, quasi horizontal sliding motion (Duthoit et al., 2020). Chambers were placed 7.5 cm into the ground to ensure imperviousness. The chambers had a volume varying from 0.7 to 0.9 m^3 and an area of 0.35 m^2, covering most of one quarter of the Voronoi space occupied by an individual coffee bush (Defrenet et al., 2016). A full cycle of measurements was six hours, spending one hour per chamber and alternating between the control plot *A* and the N-fertilised plot *B*. A system of air valves diverted the air from the different chambers. After changing to a new chamber, the chamber was open for the first 15 min to purge the system and assure that the pumped air was in equilibrium with ambient air. Subsequently, the chamber closed, and for the next 45 min N_2O and CO_2 concentrations in the chamber were monitored and used to calculate a flux based on non-linear curve fitting.

An Innova Photoacoustic Gas Monitor 1312i (INNOVA 1312, LumaSense Technology Inc., Denmark) continuously measured N_2O and CO_2 concentrations at 90 s intervals Liengaard et al. (2013)). The INNOVA was calibrated from the factory and validated between measurements to reach atmospheric levels. Measurement drift and gas interferences (CO_2 and $H_2O(g)$ on N_2O measurements) were taken into account in the INNOVA software and validated based on absolute gas concentration measurements using gas standards. Soil water content and soil temperature at three different depths (5, 15 and 30 cm) as well as chamber temperature were measured simultaneously with CS616 Water Content Reflectometers and thermocouples, respectively. Data were stored in a Campbell Scientific CR1000 Datalogger. The soil water content and temperature sensors were connected to the datalogger by means of two Campbell Scientific AM16/32B Relay Multiplexers.

A Campbell Scientific SDM-CD16AC channel relay controller connected to the datalogger controlled the opening and closing of the lids at specific times, and a second one controlled the airflow to and from the chambers through a system of electronically operated valves. The closure efficiency of the operating chambers was successfully validated through tests of stable N_2O and CO_2 concentrations after injecting known concentrations of N_2O and CO_2 while chambers were completely sealed off. Consistency in in-situ CO_2 concentration measurements during N_2O bursts further helped to ensure a high closure efficiency during measurement campaigns.

Measurements of N_2O fluxes during the full measurement period (with the exception April to November 2017 and March and April 2018) were subsequently used to calculate a mean annual N_2O fluxes for ambient and N-fertilised plots, respectively. Fluxes were integrated over time and mean values were calculated per month to avoid biased results due to data gaps.

2.3. N_2O and CO_2 fluxes along a slope

Twenty-five static chambers were distributed over five plots along a slope in field *(C)* (Fig. 1). The chambers were made of PVC and including a sealed non-transparent lid with a gas septum to create a gastight chamber. Chambers were left open except during measurements. The chamber volume was 0.68 l covering an area of 77 cm^2 and placed three centimetres into the soil. Five gas samples were collected at regular intervals from each chamber within 45 min after the chambers had been closed. This was repeated in 11 campaigns made between 8AM and 8PM. The samples of 12 ml were taken with a syringe and immediately transferred to 6 ml pre-evacuated glass vials (Flat Bottom Soda Vials,

Labco, United Kingdom), and later analysed for CO_2 and N_2O in a gas chromatograph with an electron capture detector (SRI 310 C) and according to Ekeberg et al. (2004). Fluxes were finally calculated based on the linear change in gas concentrations over time (Ambus et al., 1993).

2.4. Soil sampling and analyses

Soil samples were taken with an Edelman auger Ø7 20 cm within a meter from both the automatic chambers and the static chambers at 10, 15, 20, 30, and 40 cm depth in fields *A* and *B* and at 10 cm depth in field *C*. Sampling dates covered the periods just before and after fertilisation events: soil samples in fields *A* and *B* were taken in the following time periods: 12–05–2016 to 27–07–2016, 17–02–2017 to 05–03–2017, 13–02–2018 to 08–03–2018 and 24–08–2018 to 11–09–2018. Soil samples from field *C* were taken from 28 to 08–2018 to 11–09–2018.

Soil parameters including bulk density (g cm^{-3}), total content of N (%), total organic C content (%), pH, Cation Exchange Capacity (CEC) (cmol kg^{-1}), base saturation (BS, %) and nutrients including Ca, Mg, K, and Na (cmol kg^{-1}) from fields *(A)* and *(B)* were determined on soil samples collected on 29–03–2016. Bulk density was determined on soil cores collected with 100-cm^{-3} volumetric cylinders and dried at 105 °C. Soil samples were dried at 40 °C, homogenised, sieved (2 mm) and analysed for total C and N by total combustion using an automatic analyser Thermo Finnigan FlashEA 1112 (Waltham, Massachusetts, USA). Soil pH was measured in water after air drying and sieving the sample (2 mm). Measurements were done in a 1:2.5 ml ratio, using a potentiometer. CEC was determined by extraction with 1 M ammonium acetate solution at a pH of 7.0. Exchangeable cations Ca, Mg, K and Na were analysed with 1 M ammonium acetate.

For inorganic nitrogen measurements in the soil samples, 10 g of fresh soil was mixed with 100 ml 1 M KCl, shaken for one hour and centrifuged at 28 rounds per second for 15 min. Supernatants were filtered through paper filters, then again through filters of 0.45 μm pore size. For fields *(A)* and *(B)*, soil NO_3^- and NH_4^+ concentrations were measured by titration with MgO and reduction of NO_3^- to NH_4^+ with Devarda's alloy. Average concentrations of NO_3^- and NH_4^+ in the soil were calculated from six replicates per sampling round and per depth interval. The NO_3^- to NH_4^+ concentrations were finally calculated as mg N per kg dry soil. The detection limit was calculated to be 0.6 mg N kg^{-1}. The NO_3^- concentrations of the soil samples from field *C* were measured using ion chromatography (Metrohm, Herisau Switzerland).

Volumetric soil moisture (in % v/v) from each plot along the slope (field C) was determined by using a ML2X Theta Probe coupled to an HH2 Moisture Meter (Delta-T Devices, Cambridge, UK).

2.5. Regional study sites and incubation experiment

In order to determine spatial variations in production of N_2O and CO_2 at a regional scale, soil samples were collected from five different coffee farms located on well drained soils in central Costa Rica during the period 01–09.11.2018 (Fig. 1; Table 1).

Five soil cores of 8 × 8 cm from soil surface to the depth of eight centimetres were collected from each of the five study sites *I to V*. The 25 soil cores were collected close to the trunk of coffee trees, however, still at a distance so that the root system was not unnecessarily disturbed. The moisture level in the soil cores were kept constant and the soil was kept cool until laboratory work was conducted. Each soil core was divided into four smaller soil cores by using PVC pipes with a diameter of 2.8 cm, a height of 7 cm, a surface area of 6.16 cm^2 and a volume of 43.12 cm^3. Each of the smaller soil cores received a different treatment: i) drainage and no fertiliser (the control), ii) drainage and application of NH_4NO_3, iii) drainage and application of KNO_3, and finally iv) water saturation with application of KNO_3. The intention behind implementing drained and water saturated treatments was to illustrate varying topography and variation from dry and rainy seasons. The applied amount of fertiliser in the form of NH_4NO_3 or KNO_3 was equivalent to

Table 1
Study site characteristics. All study sites are planted with Coffea arabica var. Caturra or var. Catuai.

Study site	Location	Elevation (m ASL)	Precip. rate (mm yr^{-1})	Avg. an. air temp. (°C)	Soil type (USDA ST)	N-fertiliser (kg ha^{-1} yr^{-1})
I AEC	Aquiares Estate Coffee, Turrialba, Cartago (09°56′19″N, 83°43′46″W)	800–1300	3000	19.5	Andisol	250
II FLH	Finca La Hilda, Poás, Alajuela (10°05′31.9″N, 84°13′57.7″W)	1400	2500	20	Andisol	*Unknown*
III FC	Finca Canuela, Naranjo, Alajuela (10°08′46.5″N, 84°24′45.4″W)	1300	2500	20	Andisol	*Unknown*
IV TEC	Tarrazú Estate Coffee, Tarrazú, San José (09°39′30.6″N, 84°02′42.6″W)	1400–1900	1500	18.5	Ultisol	425–450
V CAT	CATIE, Turrialba, Cartago (09°53′44″N, 83°40′7″W)	660	3200	23.5	Inceptisol	300

40 kg N ha^{-1} and 90 kg N ha^{-1} respectively. Following fertilisation, 20 ml of water was added to each of the drained samples whereas the water saturated samples were added water to the edge of the soil core to ensure saturation. The soil cores were then incubated for a period of 7 days at 20 °C. N$_2$O and CO$_2$ gas fluxes were estimated at days one (the

day of treatment), three, and seven as follows: The incubation chambers were sealed during 1 h. Four gas samples of 6 ml were taken from each incubation chamber over the course of 1 h, with 20 min intervals. The gas samples were analysed for N$_2$O and CO$_2$ in a gas chromatograph with an electron capture detector (SRI 310 C). Fluxes were calculated from
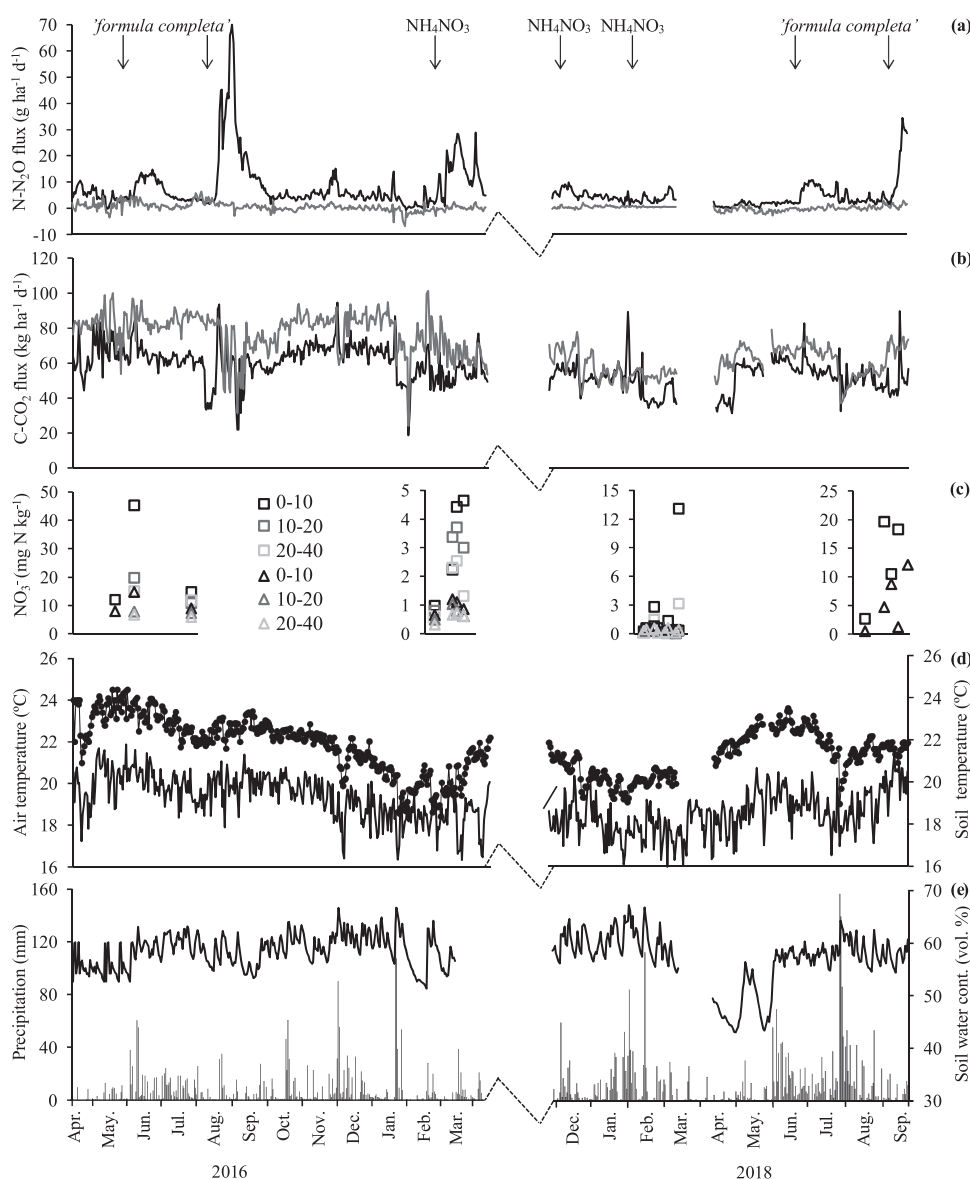

Fig. 2. (a) and (b) N$_2$O fluxes (g ha^{-1} d^{-1}) and CO$_2$ fluxes (kg ha^{-1} d^{-1}) from the control plot (grey lines) and the N-fertilised plot (black lines) in study site I. Arrows mark the days of fertilisation, types of N-fertiliser are noted above. (c) soil water concentrations of NO$_3$ (mg N kg^{-1}) from the control plot (triangles) and the N-fertilised plot (squares) in study site I, at the depth intervals 0–10, 0–15, 10–20, 15–30 and 20–40 centimetres below soil surface. (e) air and soil temperature (°C) shown with line and markers, respectively (f) daily precipitation (mm) shown with a line measured in field (C) and soil water content shown as bars (vol%). Soil gas fluxes, soil temperatures and soil water content were measured continuously during the full measurement period with the exception April to November 2017 and March and April 2018.

the regression slope. At the end of incubation, soil samples were analysed for soil water content, soil organic C content, soil water NO_3 concentrations, and soil water pH. Soil water content was determined by the difference in weight before and after 24 h of drying at 105 ºC. The soil organic C content was found by using a CS 500-analyzer heated to 1350 ºC and calibrated to carbon-standards where after the soil organic C content was determined using an infrared detector after burning the soil. Soil water pH was measured in a mix of 10 g soil with 25 ml of distilled water at room temperature and after shaking for 50 min and centrifuging for five minutes until the soil had settled. The supernatants were filtered and soil NO_3 concentrations were analysed using ion chromatography (Metrohm, Herisau Switzerland).

The measured gas concentrations of N_2O and CO_2 in ppm were converted to µmol m^{-3} by using the ideal gas law as presented by Jørgensen and Elberling (2012). Daily flux rates (µg N-N_2O m^{-2} d^{-1} for the in situ measurements, µg N-N_2O g^{-1} d^{-1} for the incubated soil samples) were then calculated from the slope of a linear regression model.

2.6. Statistical analyses

One-way analysis of variance (ANOVA) and the Student's t test were used to determine statistically significant differences. Relationships between various variables were determined by Pearson's correlation coefficients (r) using a two-tailed test. The level of significance was 0.05.

3. Results

3.1. In-situ continuous measurements (AEC site)

3.1.1. Climate

Throughout the entire measurement period, the highest precipitation rates were measured in January and July. Annual precipitation rates were 2191 mm in 2016, 2069 mm in 2017 and 3014 mm in 2018 (Fig. 2). The highest air temperatures were measured from April to June and from August to October and the lowest temperatures (°C) were measured from December to March. No significant (p > 0.05) variations were seen in monthly temperatures ranging from 18.0 ± 0.2 to 20.7 ± 0.1 °C nor the annual average air temperatures between 2016 (19.5 ± 0.4 °C), 2017 (19.3 ± 0.3 °C), and 2018 (19.4 ± 0.4 °C) (Fig. 2).

3.1.2. Soil water content and soil temperature

Soil water content varied between 43.0 ± 0.4 and 77.0 ± 0.5% by volume (2016–2018) with no significant (p > 0.05) differences between treatments. Soil water content noticeably increased after heavy rainfall (Fig. 2). Monthly average soil temperatures ranged from 19.7 ± 0.7 °C to 23.7 ± 0.1 °C from 2016–2018. The highest soil temperatures were observed in May and June 2016 and the lowest soil temperatures in January and February 2017 (Fig. 2).

3.1.3. Soil characteristics

Soil characteristics are summarized in Table 2. Soil pH was slightly acidic in all depths while all other parameters decreased with depth as expected. No significant (p > 0.05) differences in CEC, Mg or Na were found between the N-fertilised plot and the control plot. The content of K differed significantly between the two plots. The N and C contents in the N-fertilised plot were similar to the control plots found and in both cases decreasing with depth. The C:N ratio varied between 10.6 and 11.9 in the control plot whereas the C:N ratio in the N-fertilised plot varied from 11.4 at the depth of 10 cm to 12.9 at the depth of 40 cm.

3.1.4. Soil water concentrations of NO_3 and NH_4^+

Soil water concentrations of NO_3 and NH_4^+ in the N-fertilised plot varied from 0 ± 0.01–45.4 ± 11 mg N kg^{-1} and from 0 ± 0.01–16.41 ± 5.49 mg N kg^{-1} soil, respectively. Soil water concentrations of NO_3 and NH_4^+ in the control plot varied from 0.11 ± 0.13–19.63 ± 9.63 mg N kg^{-1} and from 0 ± 0.01–7.4 ± 0.6 mg N kg^{-1}, respectively. Significant (p < 0.05) differences in the concentrations of both NO_3 and NH_4^+ were observed between the four measurement periods in all depth intervals. The highest concentrations of NO_3 were measured after the May 2016 fertilisation with *'formula completa'* whereas the lowest concentrations were measured after the February 2017

Table 2

Chemical soil characteristics from the control plot, field A, and the N-fertilised plot, field B, in study site I measured in 2016.

Study site *(I) AEC*					
Control plot - field *(A)*					
Depth (cm)	**pH** H$_2$O	**CEC**	**Ca**	**Mg**	**K**	**Na**
		---------	---------	-- (cmol kg^{-1}) --	---------	---------
0 - 10	5.1 ± 0.1	53.2 ± 2.4	9.7 ± 2.4	1.9 ± 0.2	1.0 ± 0.1	0.1 ± 0.0
10 - 20	4.9 ± 0.1	48.6 ± 1.3	2.5 ± 1.3	0.6 ± 0.1	0.6 ± 0.1	0.0 ± 0.0
20 - 40	5.0 ± 0.1	47.1 ± 0.9	2.3 ± 0.6	0.6 ± 0.1	0.6 ± 0.1	0.0 ± 0.0
Depth (cm)	**BS**	**C**	**N**	**C:N ratio**	**Bulk density (g cm^{-3})**	
	---------- % ----------					
0 - 10	23.8 ± 1.1	8.5 ± 0.6	0.8 ± 0.1	10.6	0.7	
10 - 20	7.8 ± 0.4	6.1 ± 0.3	0.6 ± 0.0	11.0	0.7	
20 - 40	7.5 ± 0.4	5.3 ± 0.0	0.5 ± 0.0	11.9	0.8	
N-fertilised plot - field *(B)*					
Depth (cm)	**pH** H$_2$O	**CEC**	**Ca**	**Mg**	**K**	**Na**
		---------	---------	-- (cmol kg^{-1}) --	---------	---------
0 - 10	5.5 ± 0.2	52.6 ± 0.8	15.9 ± 2.4	1.2 ± 0.2	1.2 ± 0.2	0.1 ± 0.0
10 - 20	5.1 ± 0.2	46.2 ± 1.1	4.0 ± 0.9	0.8 ± 0.2	0.8 ± 0.2	0.0 ± 0.0
20 - 40	5.0 ± 0.3	45.0 ± 0.6	2.8 ± 0.4	0.6 ± 0.1	0.8 ± 0.1	0.0 ± 0.0
Depth (cm)	**BS**	**C**	**N**	**C:N ratio**	**Bulk density (g cm^{-3})**	
	---------- % ----------					
0 - 10	35.5 ± 0.8	7.9 ± 0.25	0.7 ± 0.0	11.4	0.7	
10 - 20	12.3 ± 0.3	5.3 ± 0.41	0.5 ± 0.0	11.8	0.7	
20 - 40	9.3 ± 0.5	4.5 ± 0.22	0.4 ± 0.0	12.9	0.8	

fertilisation with NH_4NO_3. The highest concentrations of NH_4^+ were measured after the January 2018 fertilisation with NH_4NO_3 in the plantation, and the lowest concentrations of NH_4^+ were measured after the February 2017 fertilisation with NH_4NO_3 (Fig. 2). The concentrations of NO_3^- and NH_4^+ measured after fertilisation were significantly ($p < 0.05$) higher than before fertilisation in the N-fertilised plot and the highest concentrations were measured in the first ten centimeters below soil surface.

3.1.5. Soil N_2O and CO_2 fluxes

Daily N_2O fluxes from the control plot were low varying from -6.8 ± 1.0–6.4 ± 1.1 g N-N_2O ha^{-1} d^{-1} whereas fluxes from the N-fertilised plot were significantly ($p < 0.05$) higher varying between -1.0 ± 1.4 and 70.0 ± 9.6 g N-N_2O ha^{-1} d^{-1}. A sharp increase in N_2O fluxes can be seen after fertilisation events. However, the increase varied significantly ($p < 0.05$) between fertilisation events. The highest fluxes were observed following the August 2016 fertilisation with 'formula completa' (70.0 ± 9.6 g N-N_2O ha^{-1} d^{-1}) and the February 2017 fertilisation with NH_4NO_3 (28.9 ± 4.3 g N-N_2O ha^{-1} d^{-1}). The lowest emission rates were seen after the January 2018 fertilisation with NH_4NO_3. N_2O emissions remained high up to 20 days after fertilisation and reached a stable mean level 40–48 days after fertilisation. Short bursts of N_2O fluxes were also seen when soil water increased suddenly in one case directly due to a heavy precipitation events (Fig. 2). Other less intense rain events did not result in a N_2O burst, which could be due to the absence of available nitrate in the soil or that the remained well aerated despite of the rain.

Daily CO_2 fluxes from the N-fertilised plot and the control plot ranged from 31.5 ± 4.0 to 94.4 ± 8.1 C-CO_2 kg ha^{-1} d^{-1} and from 31.4 ± 2.4–101.2 ± 3.6 C-CO_2 kg ha^{-1} d^{-1}, respectively, and were not significantly different from each other (Fig. 2). There was no significant correlation between the CO_2 fluxes and N_2O fluxes. Also, increased N_2O fluxes in the N-fertilised plot coincided with increased soil water concentrations of NO_3^- (Fig. 3).

3.2. In-situ measurements along a slope

3.2.1. Soil water content

The highest soil water content was found in plot *V* at the bottom of the slope varying from 117.4 ± 3.2–$126.9 \pm 8.2\%$ by weight, whereas the lowest soil water content was found in plot *II* at the upper part of the slope varying from 61.7 ± 1.8–$94.0 \pm 1.4\%$ by weight. No significant variations were seen between the soil water content from plots *I* to *IV*, whereas the soil water content in plot *V* was significantly ($p < 0.05$) higher (Fig. 4).

3.2.2. Soil water NO_3^- concentrations

Three days before fertilisation the soil water concentrations of NO_3^- in plots *I* - *IV* varied between 2.5 ± 0.5 and 10.9 ± 0.9 mg N kg^{-1} whereas the concentrations measured in plot *V* at the bottom of the slope were significantly ($p < 0.05$) higher, 22.3 ± 3.3 mg N kg^{-1}. The soil water NO_3^- concentrations increased after fertilisation in all five plots peaking between 18 and 32 days after fertilisation with maximum concentrations ranging from 76.4 ± 15.2–111.1 ± 9.9 mg N kg^{-1} within all five plots. Significant ($p < 0.05$) variations in the concentrations of soil water NO_3^- were measured within the entire measurement period concurrently with increases and decreases in soil water content (Fig. 4). At the end of the measurement period 40 days subsequent fertilisation, the concentrations of NO_3^- in the soil water ranged from 42.7 ± 12.2–85.8 ± 6.5 mg N kg^{-1} with the highest concentrations found in plot *III* at the middle of the slope and the lowest found in plot *IV*, respectively.

3.2.3. Soil gas fluxes

N_2O fluxes measured before fertilisation ranged from 10.0 ± 2.5–65.8 ± 19.6 g N-N_2O ha^{-1} d^{-1} within the five plots along the slope. The lowest flux rates were measured in plot *I* at the top of the

slope and plot *II* located at the upper part of the slope whereas the highest flux rate was measured in plot *V* at the bottom of the slope. Increasing N_2O flux rates were seen immediately after fertilisation in each plot. The highest flux was measured in plot *V* 11 days after fertilisation (336.1 ± 104.1 g N ha^{-1} d^{-1}) (Fig. 4). The increasing flux rates occurred in parallel with increases in soil water content due to numerous consecutive days with precipitation (Fig. 4). In plot *I* at the top of the slope and in plot *III* at the middle of the slope decreasing flux rates were measured five days after fertilisation, whereas decreases in flux rates measured in plot *II* at the upper part of the slope and in plots *IV* and *V* at the slope bottom did not occur until 11 days after fertilisation. Unexpected, nitrate levels remained high at plot II in contrast to plot I. Total N_2O emission from plots *I* and *II* at the top of the slope ranged from 2.9 ± 0.1–3.7 ± 0.1 kg N-N_2O ha^{-1}, and increased significantly to 7.3 ± 0.9 and 7.6 ± 1.2 kg N-N_2O ha^{-1} at plots *III* and *IV*, respectively. The total N_2O emission from plot *V* at the slope bottom, 9.6 ± 1.2 kg N-N_2O ha^{-1}, was significantly higher ($p < 0.05$) than the emissions from the other plots (Fig. 5).

Four days prior to fertilisation the CO_2 emission rates for all five plots were ranging between 49.2 ± 6.3 and 64.2 ± 3.13 kg C-CO_2 ha^{-1} d^{-1}. Following fertilisation, the flux rates increased for all five plots ranging from 69.8 ± 5.9–95.2 ± 5.0 kg C-CO_2 ha^{-1} d^{-1} until a sudden decrease was seen over a period of 30 days. By the end of the measurement period, the CO_2 fluxes reached a level of 48.3 ± 6.2–81.8 ± 11.1 kg C-CO_2 ha^{-1} d^{-1}. The emission rate in plot *IV* was significantly ($p < 0.05$) higher compared to the emission rates in the four other plots (Fig. 4).

3.3. Variations in soil gas fluxes from various coffee production systems

3.3.1. Soil water NO_3^- concentrations

The soil water concentrations of NO_3^- ranged from 36.4 ± 7.3–124.9 ± 4.7 mg N kg^{-1} within the five different study sites in the central Costa Rica (Table 3). Soil pH was found to be near-neutral to acidic among all study sites ranging from 4.8 ± 0.1–6.8 ± 0.1 with the lowest pH value measured on an Ultisol in study site *(IV) TEC* and the highest pH value measured on an Inceptisol in study site *V*. Distinct variations were found in the soil C content within all study sites varying from 2.4 ± 0.4–$12.4 \pm 0.7\%$. No significant ($p > 0.05$) variations in the soil water content were measured between study sites *II an V*, which were ranging from 21.8 ± 0.6–27.2 ± 2.6 vol%. The soil water content measured in study
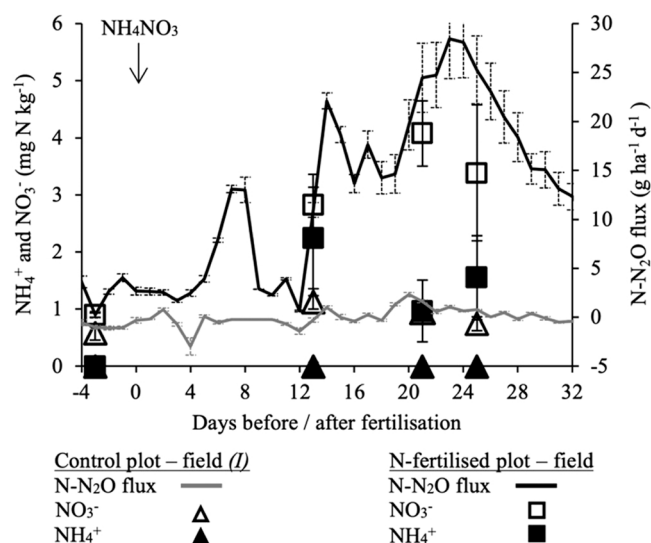

Fig. 3. Specification of soil water concentrations of NO_3^- and NH_4^+ (mg N kg^{-1}) in the root zone at the depth of 0 – 20 cm and N_2O fluxes (g ha^{-1} d^{-1}) from the control plot (field A) and the N-fertilised plot (field B) in study site (I) AEC in relation to the February 2017 fertilisation with NH_4NO_3. Day of fertilisation marked with an arrow and marked as a zero on the x-axis.
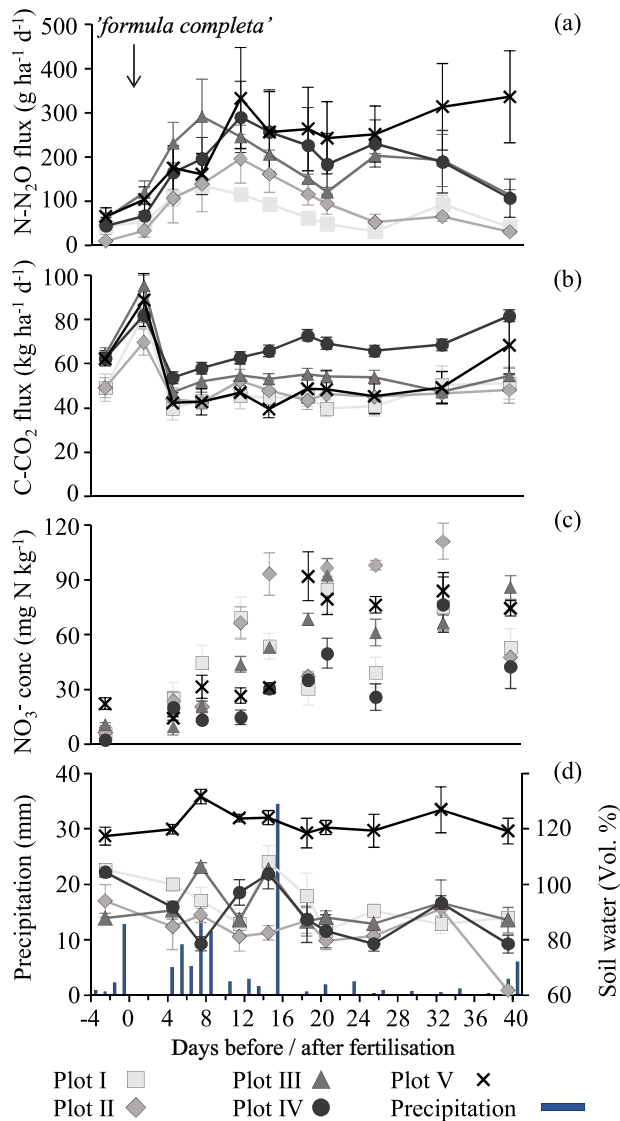
Fig. 4. (a) and (b) N_2O fluxes (g N ha^{-1} d^{-1}) and CO_2 fluxes (kg C ha^{-1} d^{-1}) from plots I to V along the slope. (c) soil water concentrations of NO_3^- (mg N kg^{-1}) at depth 0–10 cm from plots I to V. (d) daily precipitation rates (mm) measured in field) and soil water content (vol%) from plots I to V. Plot I is located at the top of the slope and plot V at the bottom of the slope. Plots II - IV are located equidistantly between the plots at the top and at the bottom of the slope. The day of fertilisation is marked as a zero on the x-axis and shown with an arrow.

site *I* were on the contrary approximately twice as high measured to be 53.5 ± 3.4 vol% (Table 3).

3.3.2. Soil type specific N_2O release over time

In general, low rates of released N_2O were found in the soil samples from the five different study sites on the same day as the fertiliser treatment was applied (Fig. 6). The highest rates were measured from the control sample from study site *I*, 0.014 ± 0.004 µg N per g dry weight (gdw^{-1}) d^{-1}, and the undrained sample treated with KNO_3 from study site *IV* (0.018 ± 0.002 µg N gdw^{-1} d^{-1}). Distinct low releases were measured from study site *III* and *V*, and no releases were measured based on three treatment types in study site *II*. The N_2O release rates measured on day three after sampling had increased and for all treatments and study sites, the release rates of N_2O were approximately twice as high as the previously measured (Fig. 6). Highest N_2O release rates were generally measured from soil samples treated with NH_4NO_3 and
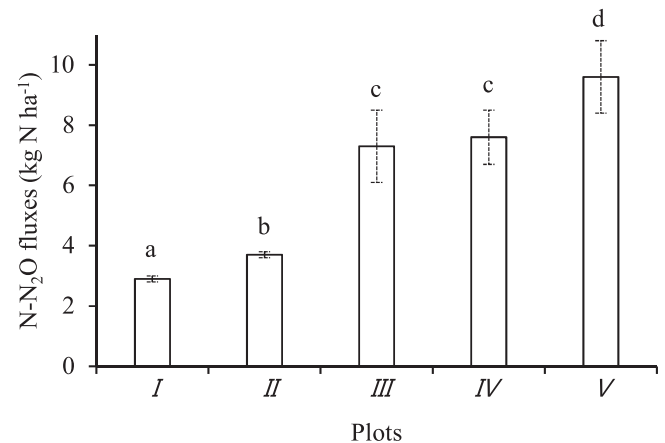
Fig. 5. Total N_2O emissions (kg N ha^{-1}) from plots I to V within field C from the day of fertilisation to 39 days after fertilisation. Letters above the bars indicate significant differences between plots ($p < 0.05$).

from undrained soils treated with KNO_3 ranging from 0.005 ± 0.002–0.045 ± 0.003 µg N gdw^{-1} d^{-1} and from 0.001 ± 0.00–0.030 ± 0.010 µg N gdw^{-1} d^{-1}, respectively. Seven days after the first measurements the N_2O release rates had again increased ranging from 0.005 ± 0.001–1.761 ± 0.236 µg N gdw^{-1} d^{-1} except for particularly the release rates from study site *IV* where decreasing rates were found during all treatments except from the undrained soil treated with KNO_3 (Fig. 6).

The total of released N_2O over all three measurement days varied widely and significantly between study sites as well as within study sites between treatments (Table 4). The treatment showing the highest total releases of N_2O was KNO_3 under undrained conditions, while study site *I* had the highest total release of N_2O among all sites, regardless of treatment.

4. Discussion

4.1. Continuous N_2O measurements and N budget

The difference between emitted N_2O from the control plot and the N-fertilised plot highlights the "N-fertiliser-induced" N_2O emission (Fig. 2a). The average annual N_2O emissions from the control plot and the N-fertilised plot were 0.2 kg N ha^{-1} and 3.1 kg N ha^{-1}, respectively. Such differences in annual N_2O emissions should be considered in the light of an overall N budget despite the fact that such budgets often and also in our case are incomplete.

Based on all known input and output of N compounds, a simplified nitrogen (N) budget is introduced. N inputs include N_2 by biological nitrogen fixation (BNF), wet NO_3^- deposition via precipitation, dry NH_4^+ deposition by dust, plant litter, and applied fertiliser. N outputs include yield loss, N_2O and N_2 loss to the atmosphere, NO_3 leaching, and NH_3 volatilization due to applied N-fertiliser. The annual sum of fertiliser-induced N_2O emission based on measurements from 12 months (April 2016 to March 2017) were used as an estimate of annual N_2O output. The N input via fertiliser rated 230 kg N-fertiliser per hectare distributed over three fertilisation events in May 2016, August 2016, and February 2017. The annual N losses from coffee harvest were 79 and 83 kg N ha^{-1} from fields *A* and *B*. Exported wood from coffee pruning adds another 40 kg N ha^{-1} y^{-1} (Charbonnier et al., 2017; Cambou et al., 2021). The plots included in this study did not include shade trees, but nearby plots were shaded with *Erythrina poeppigiana*, a popular nitrogen-fixing shade tree in the country. Annual N turnover from *Erythrina poeppigiana* pruned twice annually was estimated by Russo and Budowski (1986) to be 228 kg N ha^{-1} based on 280 trees per hectare. In a fertilised plot, about 15% of this N (34 kg N ha^{-1}) is expected to come from biological

Table 4

Total release of N_2O (μg N gdw^{-1}) from soil samples from study sites I to V incubated with no amendment (Control) or following amendment with NH_4NO_3, KNO_3 under drained conditions, or KNO_3 under undrained conditions. NH_4NO_3 or KNO_3 amendments were equivalent to 40 kg N ha^{-1} and 90 kg N ha^{-1}, respectively.

Study site	Treatment			
	Control	NH_4NO_3	KNO_3 (drained)	KNO_3 (undrained)
I	0.08 ± 0.07	0.4 ± 0.28	3.18 ± 1.97	4.5 ± 0.38
II	0.01 ± 0.00	0.03 ± 0.01	0.01 ± 0.00	0.21 ± 0.15
III	0.03 ± 0.01	0.05 ± 0.01	0.02 ± 0.00	1.85 ± 0.91
IV	0.06 ± 0.07	0.22 ± 0.1	0.04 ± 0.04	0.95 ± 1.01
V	0.00 ± 0.04	0.28 ± 0.17	0.11 ± 0.13	0.22 ± 0.22

soil temperatures can affect N_2O emissions linked to the temperature-dependence of microbial activity; which agrees with the fact that denitrification is particularly sensitive to increasing soil temperatures (Butterbach-Bahl et al., 2013). This has been observed in other tropical systems (Yamamoto et al., 2014; Han et al., 2013). Relatively high soil temperatures can stimulate a turnover of nitrate (NO_3^-) and ammonium (NH_4^+) pools and contribute to increasing N_2O emissions. In accordance with Zhu et al. (2015), higher N_2O emissions were observed during the warmer months than during the colder months indicating that the warmer temperatures might facilitate the prevalence and activities of N_2O-producing microbes, i.e. nitrifying and/or denitrifying microorganisms depending on the water content and oxygen availability.

In relation to fertilisation events during the measurement period from 2016 to 2018, high soil N_2O fluxes were observed in periods with high soil water content but also drier periods as long NO_3^- and NH_4^+ were available in soil water (Fig. 2). Since the soil moisture content was lower during the drier periods, the denitrification process was probably relatively inactive during this period which amongst other factors can explain the lower N_2O emission rates. However, N_2O emissions were still observed in the drier periods and considered to be a result of nitrification of NH_4^+ present in the aerobic soil. At the end of the drier period in March 2017, increasing N_2O fluxes were observed as a consequence of sudden and heavy precipitation. Likewise, sudden and heavy precipitation on well-drained soils can cause anaerobic conditions of short duration which increases denitrification rates and may result in short-lived high N_2O flux rates. Based on a study undertaken in a Chinese rubber plantation, Werner et al. (2006) state that short-term changes in N_2O emissions from tropical soils closely follow changes in soil moisture. Such 'hot moments' for N_2O emissions requires special attention on how to measure and how to scale integrated N_2O emissions over time.

4.2. Landscape slope controls of soil water NO_3^- concentrations and soil N_2O emissions

Increasing soil water concentrations of NO_3^- and N_2O emission rates were seen immediately after fertilisation in plot *I* at the top of the slope to plot *III* at the middle of the slope, whereas increasing soil water concentrations of NO_3^- and N_2O emission rates were delayed further down the slope. As it takes time for the N-fertiliser to seep into the soil and to be transported down-slope after the precipitation events a delay in increasing soil NO_3^- concentrations and the resultant N_2O emissions was expected. Approximately a week after fertilisation, the highest fluxes were consistently observed at the lower part of the slope, which is aligned with the destination of NO_3^- transport along the slope as well as corresponding high levels of NO_3^- and the highest soil water content promoting denitrification. Given that the area is belonging to a highly pervious watershed where 67% of rainfall is driven through the aquifer (Gómez-Delgado et al., 2011), it is likely that the end destination of NO_3^-

is the aquifer first, then the streamflow.

During the full measurement period, a general pattern indicated a relation between soil water content, NO_3^- availability and emitted N_2O. Decreasing N_2O emissions from plots *I* to *IV* were seen concurrently with decreasing soil water content whereas an increase in emitted N_2O from plot *V* at the bottom of the slope was seen despite the decreasing soil water content. A similar pattern is presented in the studies of Vilain et al. (2010) and Ashiq et al. (2021) in which the highest N_2O emissions were generally seen at the end of the slope where high soil water content appeared. This implies that the relation between topography and hydrological processes plays an essential role to the extent of soil N_2O emissions as concluded from other very different ecosystems (e.g. Peralta et al., 2016). However, the correlation between available soil water concentrations of NO_3^- and emitted N_2O is on the contrary not as evident in the plots located in the central part of the slope, which indicates that emitted N_2O was affected by other factors than available NO_3^-. The total N_2O emission from plot *V* at the bottom of the slope was more than three times higher than the total emissions from plots *I* and *II*. Taking into account the effect of topography on N_2O emissions reported here, the emitted N_2O from fields A and B is not representative for the total emitted N_2O along the entire slope.

4.3. N_2O fluxes from various coffee production systems

Undrained conditions increased N_2O emission rates from incubated soil samples from the five coffee production systems in the central highland in Costa Rica. This is supported by the studies of Hansen et al. (2014) who presented N_2O bursts under temporarily flooded agricultural land. On the contrary, the study of Liengaard et al. (2013) on South American tropical wetland soil showed higher soil water NO_3^- contents and resulting N_2O emissions in drained soil than in undrained soil, indicating potential dynamic shifts between the nitrification and denitrification processes. The largest difference in the total release of N_2O

Table 5

Annual N-budget for the control plot (A) and the N-fertilised plot B in study site I. Parameters measured in this study are underlined. Other numbers are estimates based on other studies. Arrows indicate the way in and out of the ecosystem.

		Control plot - field *A*	N-fertilised plot – field *B*
Input		BNF 114 kg N ha^{-1}	BNF 34 kg N ha^{-1}
		NO_3^- wet deposition	NO_3^- wet deposition
		NH_4^+ dry deposition	NH_4^+ dry deposition
			N-fertiliser 230 kg N ha^{-1}
Output	→	Harvest 79 kg N ha^{-1}	Harvest 83.1 kg N ha^{-1}
		Wood export 40 kg N ha^{-1}	Wood export 40 kg N ha^{-1}
	↑	N_2O 0.2 kg N ha^{-1}	N_2O 3.1 kg N ha^{-1}
		N_2 denitrification	N_2 denitrification
		NH_3 volatilisation	NH_3 volatilisation
	↓	NO_3^- leaching	NO_3^- leaching 67 kg N ha^{-1}

between the undrained and drained soil samples were observed for study site *III* treated with KNO_3, indicating that the soil in this plantation has a high potential for denitrification-induced N_2O emissions. The highest N_2O release from undrained soil samples was found in soil from study site *I*. This can be due to the high content of organic carbon (12.4%) at the study site, which in combination with high levels of available NO_3 and soil water compared to the four other sites can lead to high releases of N_2O due to increasing denitrifying activity.

Study sites *I - III* are located on moderately acidic Andisols, pH ranging from 5.3 ± 0.1–5.9 ± 0.1, whereas study sites *IV* and *V* are located on a more acidic Ultisol (pH 4.8 ± 0.1) and a near-neutral Inceptisol (pH 6.8 ± 0.1). The highest total release of N_2O were seen from study sites *I* and *III* located on Andisols and from study site *IV* located on an acidic Ultisol. Low soil pH favours the formation of N_2O from denitrification (e.g. Bremner, 1997, Myhre et al., 2013, Van Den Heuvel et al., 2011). As the soil pH at study site *IV* is rather acidic this can lead to higher emission rates. Additionally, the soil type is an Ultisol, which appears to be more compact and wetter, which can imply that local reduced conditions favouring higher denitrification rates may be more common compared to the other soil types present in this study. Studies of Bouwman et al. (1993) and Ishizuka et al. (2005) showed that N_2O emissions differed according to soil type with the highest emissions rates observed in a rubber plantation and an oil palm plantation located on an Ultisol with WFPS of 55.3% and 73.1%, respectively (Ishizuka et al., 2005).

The highest rates of N_2O release were observed seven days after treatment whereas low rates were observed on the day of treatment and three days subsequent to the treatment. On day seven, the highest rates were seen based on treatment with KNO_3 under undrained conditions while on day three elevated rates of released N_2O were in general based on treatment with NH_4NO_3 which may be due to nitrification as the conditions presumably were aerobic and hence NH_4^+ was transformed in to NO_2^- followed by NO_3^- with N_2O as a by-product (Butterbach-Bahl et al., 2013).

5. Conclusions and implications

This study investigates the temporal and spatial controls of N_2O emissions from coffee production systems in Costa Rica. The following main conclusions can be made:

(I) Continuous field measurements of N_2O emissions and the availability of soil NO_3 and soil water content indicate that N_2O emissions from the fertilised coffee production system studied at site 1 are related to hot moments, driven by the combination of factors, including high water content and nitrate concentrations, which can partly be explained by the timing of fertilization, the amount and type of fertiliser as well as major precipitation events. The majority (80%) of the annual N_2O is released in short-term hot moments of two to three weeks duration, three times annually. This means that an annual N_2O budget without including these bursts (in total seven to eight weeks) but only including the remaining 44 weeks will markedly underestimate the annual N_2O emission.

(II) Local hydrology within individual fields is crucial for mobilising nitrate along water flow patterns downhill (surface or near-surface flow) which can result in potential hotspot areas in depressions or lowlands within fields. Such hotspots are characterized by poor drainage conditions, high water contents, high nitrate concentrations derived from runoff from the slope which creates environmental conditions favouring denitrification and hence high N_2O emissions. Site-specific measurements indicated that such hotspots not only resulted in the highest N_2O emission rates along the slope, but also extended the period of high emission rates for several weeks longer than the general well-drained slope due to a continuous input of NO_3 from the slope.

(III) The awareness of N_2O bursts associated with fertilisation and precipitation events as well as hotspot areas in the least well-drained parts of the coffee production systems are not included in current

annual estimate of N_2O emissions from coffee production. This leads to our conclusion that N_2O emissions from coffee production systems may currently be underestimated and should be better constrained by quantifications of both N_2O hotspots and hot moments.

(IV) Implications of this work in order to reduce N_2O emissions remain unclear and clear recommendations should be based on additional future work. However, based on our current knowledge we speculate that improved timing and repeated fertilisation with less amount of fertiliser, slow release fertilizer or low-N_2O emitting fertilizers are expected to both increase N uptake by coffee plants, decrease N_2O emissions, decrease N flow across sloping fields, reduce NO_3 input to N_2O hotspots and save plantation owners cost for fertiliser. This may also increase labour work associated with fertilizing.

(V) Variations in N_2O production across soil types and coffee management practices urgently need to be further explored to better constrain N_2O emissions at the country level.

Although we considered nitrogen (N) dynamics in coffee plantations on a local scale, the results from our study are relevant on a larger scale and we can make overall recommendations to minimize N2O emissions, summarized as:

Reduce the application of N or add lesser amounts of N but more frequently. Choose the time for fertilisation since fertilisation prior to heavy precipitation events increases the loss of N due to denitrification and leaching. Be aware that up-hill slopes require and can leach more N than lowland areas.

Declaration of Competing Interest

The authors declare that they have no known competing financial interests or personal relationships that could have appeared to influence the work reported in this paper.

Data availability

Data will be made available on request.

References

Ambus, P., Clayton, H., Arah, J.R.M., Smith, K.A., Christensen, S., 1993. Similar N_2O flux from soil measured with different chamber techniques. Atmos. Environ. Part A. Gen. Top. 27, 121–123.

Ashiq, W., Vasava, H.B., Ghimire, U., Daggupati, P., Biswas, A., 2021. Topography Controls N_2O Emissions Differently during Early and Late Corn Growing Season. Agronomy 11 (1), 187. https://doi.org/10.3390/agronomy11010187.

Bouwman, A.F., Fung, I., Matthews, E., John, J., 1993. Global Analysis of the Potential for N_2O Production in Natural Soils. Glob. Biogeochem. Cycles 7 (3), 557–597.

Bremner, J.M., 1997. Sources of nitrous oxide in soils. Nutr. Cycl. Agroecosyst. 49 (1–3), 7–16. https://doi.org/10.1023/a:1009798022569.

Butterbach-Bahl, K., Baggs, E.M., Dannenmann, M., Kiese, R., Zechmeister-Boltenstern, S., 2013. Nitrous oxide emissions from soils: How well do we understand the processes and their controls. Philos. Trans. R. Soc. B: Biol. Sci. 368 (1621) https://doi.org/10.1098/rstb.2013.0122.

Cambou, A., Thaler, P., Clément-Vidal, A., Barthès, B.G., Charbonnier, F., Van den Meersche, K., Aguilar Vega, M.E., Avelino, J., Davrieux, F., Labouisse, J.-P., de Melo Virginio Filho, E., Deleporte, P., Brunet, D., Lehner, P., Roupsard, O., 2021. Concurrent starch accumulation in stump and high fruit production in coffee (Coffea arabica. Tree Physiol. 41, 2308–2325. https://doi.org/10.1093/treephys/tpab075.

Cannavo, P., Harmand, J.-M., Zeller, B., Vaast, P., Ramírez, J.E., Dambrine, E., 2013. Low nitrogen use efficiency and high nitrate leaching in a highly fertilized Coffea

arabica–Inga densiflora agroforestry system: a ^{15}N labeled fertilizer study. Nutr. Cycl. Agroecosyst. 95, 377–394. https://doi.org/10.1007/s10705-013-9571-z.

Capa, D., Pérez-Esteban, J., Masaguer, A., 2015. Unsustainability of recommended fertilization rates for coffee monoculture due to high N_2O emissions. Agron. Sustain. Dev. 1551–1559. https://doi.org/10.1007/s13593-015-0316-z.

Charbonnier, F., Roupsard, O., le Maire, G., Guillemot, J., Casanoves, F., Lacointe, A., Vaast, P., Allinne, C., Audebert, L., Cambou, A., Clément-Vidal, A., Defrenet, E., Duursma, R.A., Jarri, L., Jourdan, C., Khac, E., Leandro, P., Medlyn, B.E., Saint-André, L., Thaler, P., Van Den Meersche, K., Barquero Aguilar, A., Lehner, P., Dreyer, E., 2017. Increased light-use efficiency sustains net primary productivity of shaded coffee plants in agroforestry system. Plant, Cell Environ. 40, 1592–1608. https://doi.org/10.1111/pce.12964.

Chevallier, T., Fujisaki, K., Roupsard, O., Guidat, F., Kinoshita, R., de Melo Viginio Filho, E., Lehner, P., Albrecht, A., 2019. Short-range-order minerals as powerful factors explaining deep soil organic carbon stock distribution: the case of a coffee agroforestry plantation on andosols in Costa Rica. SOIL 5 (2), 315–332. https://doi.org/10.5194/soil-5-315-2019.

Danse, M., Wolters, T., 2014. Sustainable coffee in the mainstream. Greener Manag. Int. 2003 (43), 36–51. https://doi.org/10.9774/gleaf.3062.2003.au.00006.

Defrenet, E., Roupsard, O., Van den Meersche, K., Charbonnier, F., Pastor Pérez-Molina, J., Khac, E., Prieto, I., Stokes, A., Roumet, C., Rapidel, B., de Melo Virginio Filho, E., Vargas, V.J., Robelo, D., Barquero, A., Jourdan, C., 2016. Root biomass, turnover and net primary productivity of a coffee agroforestry system in Costa Rica: effects of soil depth, shade trees, distance to row and coffee age. Ann. Bot. 118, 833–851. https://doi.org/10.1093/aob/mcw153.

Duthoit, M., Roupsard, O., Crequy, N., Sauze, J., Van den Meersche, K., 2020. Conception d'un dispositif automatisé de chambres de mesures d'échanges gazeux du sol à fermeture horizontale. Cah. Des. Tech. De. l'INRA 102 (4), 19 (pp).

Ekeberg, D., Ogner, G., Fongen, M., Joner, E., Wickstrøm, T., 2004. Determination of CH_4, CO_2 and N_2O in air samples and soil atmosphere by gas chromatography mass spectrometry, GC-MS. J. Environ. Monit. 6, 621–623. https://doi.org/10.1039/b401315h.

FAO, 2018, FAOSTAT - Value of Agricultural Production. ⟨http://www.fao.org/faostat/en/#data/QV⟩.

Gómez-Delgado, F., Roupsard, O., le Maire, G., Taugourdeau, S., Pérez, A., van Oijen, M., Vaast, P., et al., 2011. Modelling the Hydrological Behaviour of a Coffee Agroforestry Basin in Costa Rica. Hydrol. Earth Syst. Sci. 15 (1), 369–392. https://doi.org/10.5194/hess-15-369-2011.

Han, W., Xu, J., Wei, K., Shi, Y., Ma, L., 2013. Estimation of N_2O emission from tea garden soils, their adjacent vegetable garden and forest soils in eastern China. Environ. Earth Sci. 70 (6), 2495–2500. https://doi.org/10.1007/s12665-013-2292-4.

Hansen, M., Clough, T.J., Elberling, B., 2014. Flooding-induced N_2O emission bursts controlled by pH and nitrate in agricultural soils. Soil Biol. Biochem. 69, 17–24. https://doi.org/10.1016/j.soilbio.2013.10.031.

Harmand, J.M., Avila, H., Dambrine, E., Skiba, U., de Miguel, S., Renderos, R.V., Oliver, R., Jimenez, F., Beer, J., 2007. Nitrogen dynamics and soil nitrate retention in a Coffea arabica-Eucalyptus deglupta agroforestry system in Southern Costa Rica. Biogeochemistry 85, 125–139. https://doi.org/10.1007/s10533-007-9120-4.

Hergoualc'h, K., Blanchart, E., Skiba, U., Hénault, C., Harmand, J.M., 2012. Changes in carbon stock and greenhouse gas balance in a coffee (Coffea arabica) monoculture versus an agroforestry system with Inga densiflora, in Costa Rica. Agric., Ecosyst. Environ. 148, 102–110. https://doi.org/10.1016/j.agee.2011.11.018.

Hergoualc'H, K., Skiba, U., Harmand, J.M., Hénault, C., 2008. Fluxes of greenhouse gases from Andosols under coffee in monoculture or shaded by Inga densiflora in Costa Rica. Biogeochemistry 89 (3), 329–345. https://doi.org/10.1007/s10533-008-9222-7.

Ishizuka, S., Iswandi, A., Nakajima, Y., Yonemura, S., Sudo, S., Tsuruta, H., Murdiyarso, D., 2005. The variation of greenhouse gas emissions from soils of various land-use/cover types in Jambi province, Indonesia. Nutr. Cycl. Agroecosyst. 71 (1), 17–32. https://doi.org/10.1007/s10705-004-0382-0.

Jørgensen, C.J., Elberling, B., 2012. Effects of flooding-induced N_2O production, consumption and emission dynamics on the annual N_2O emission budget in wetland soil. Soil Biol. Biochem. 53, 9–17. https://doi.org/10.1016/j.soilbio.2012.05.005.

Lestari, Y., Maas, A., Purwanto, B.H., Utami, S.N.H., 2016. The Influence of Lime and Nitrogen Fertilizer on Soil Acidity, Growth and Nitrogen Uptake of Corn in Total Reclaimed Potential Acid Sulphate Soil. J. Agric. Sci. 8 (12), 197. https://doi.org/10.5539/jas.v8n12p197.

Liengaard, L., Nielsen, L.P., Revsbech, N.P., Priemé, A., Elberling, B., Enrich-Prast, A., Kühl, M., 2013. Extreme emission of N_2O from tropical wetland soil (Pantanal, South America. Front. Microbiol. 3 (JAN), 1–13. https://doi.org/10.3389/fmicb.2012.00433.

Myhre, G., Shindell, D., Bréon, F.-M., Collins, W., Fuglestvedt, J., Huang, J., Koch, D., Lamarque, J.-F., Lee, D., Mendoza, B., Nakajima, T., Robock, A., Stephens, G., Takemura, T., Zhang, H., 2013. Anthropogenic and natural radiative forcing: Positive feedbacks. J. Mar. Sci. Eng. 6 (4) https://doi.org/10.3390/jmse6040146.

Peralta, A.L., Johnston, E.R., Matthews, J.W., Kent, A.D., 2016. Abiotic correlates of microbial community structure and nitrogen cycling functions vary within wetlands. Freshw. Sci. 35 (2), 573–588. https://doi.org/10.1086/685688.

Reay, D.S., Davidson, E.A., Smith, K.A., Smith, P., Melillo, J.M., Dentener, F., Crutzen, P. J., 2012. Global agriculture and nitrous oxide emissions. Nat. Clim. Change 2 (6), 410–416. https://doi.org/10.1038/nclimate1458.

Russo, R.O., Budowski, G., 1986. Effect of pollarding frequency on biomass of *Erythrina poeppigiana* as a coffee shade tree. Agrofor. Syst. 4, 145–162. https://doi.org/10.1007/BF00141546.

Sakata, R., Shimada, S., Arai, H., Yoshioka, N., Yoshioka, R., Aoki, H., Kimoto, N., Sakamoto, A., Melling, L., Inubushi, K., 2015. Effect of soil types and nitrogen fertilizer on nitrous oxide and carbon dioxide emissions in oil palm plantations. Soil Sci. Plant Nutr. 61 (1), 48–60. https://doi.org/10.1080/00380768.2014.960355.

Van Den Heuvel, R.N., Bakker, S.E., Jetten, M.S.M., Hefting, M.M., 2011. Decreased N_2O reduction by low soil pH causes high N_2O emissions in a riparian ecosystem. Geobiology 9 (3), 294–300. https://doi.org/10.1111/j.1472-4669.2011.00276.x.

Veldkamp, E., Keller, M., 1997. Nitrogen oxide emissions from a banana plantation in the humid tropics. J. Geophys. Res.: Atmos. 102, 15889–15898. https://doi.org/10.1029/97JD00767.

Vilain, G., Garnier, J., Tallec, G., Cellier, P., 2010. Effect of slope position and land use on nitrous oxide (N_2O) emissions (Seine Basin, France. Agric. For. Meteorol. 150 (9), 1192–1202. https://doi.org/10.1016/j.agrformet.2010.05.004.

Wang, C., Amon, B., Schulz, K., Mehdi, B., 2021. Factors that influence nitrous oxide emissions from agricultural soils as well as their representation in simulation models: a review. Agronomy 11, 770. https://doi.org/10.3390/agronomy11040770.

Weitz, A.M., Linder, E., Frolking, S., Crill, P.M., Keller, M., 2001. N2O emissions from humid tropical agricultural soils: Effects of soil moisture, texture and nitrogen availability. *Soil Biol. Biochem.* 33 (7–8), 1077–1093. ⟨https://doi.org/10.1016/S0038-0717⟩(01)00013-X.

Werner, C., Zheng, X., Tang, J., Xie, B., Liu, C., Kiese, R., Butterbach-Bahl, K., 2006. N_2O, CH_4 and CO_2 emissions from seasonal tropical rainforests and a rubber plantation in Southwest China. Plant Soil 289 (1–2), 335–353. https://doi.org/10.1007/s11104-006-9143-y.

Yamamoto, A., Akiyama, H., Naokawa, T., Miyazaki, Y., Honda, Y., Sano, Y., Nakajima, Y., Yagi, K., 2014. Lime-nitrogen application affects nitrification, denitrification, and N_2O emission in an acidic tea soil. Biol. Fertil. Soils 50 (1), 53–62. https://doi.org/10.1007/s00374-013-0830-6.

Yan, Y., Sha, L., Cao, M., Zheng, Z., Tang, J., Wang, Y., Zhang, Y., Wang, R., Liu, G., Wang, Y., Sun, Y., 2008. Fluxes of CH_4 and N_2O from soil under a tropical seasonal rain forest in Xishuangbanna, Southwest China. J. Environ. Sci. 20 (2), 207–215. https://doi.org/10.1016/S1001-0742(08)60033-9.

Zhou, W.J., Ji, H.L., Zhu, J., Zhang, Y.P., Sha, L.Q., Liu, Y.T., Zhang, X., Zhao, W., Dong, Y.X., Bai, X.L., Lin, Y.X., Zhang, J.H., Zheng, X.H., 2016. The effects of nitrogen fertilization on N_2O emissions from a rubber plantation. Sci. Rep. 6 (June), 1–12. https://doi.org/10.1038/srep28230.

Zhu, T., Zhang, J., Huang, P., Suo, L., Wang, C., Ding, W., Meng, L., Zhou, K., Hu, Z., 2015. N_2O emissions from banana plantations in tropical China as affected by the application rates of urea and a urease/nitrification inhibitor. Biol. Fertil. Soils 51 (6), 673–683. https://doi.org/10.1007/s00374-015-1018-z.